International Journal for Multidisciplinary Research (IJFMR)
E-ISSN: 2582-2160 ● Website: www.ijfmr.com ● Email: editor@ijfmr.com

Synthesis of CDSE and ZNSE Nanoparticles Functionalized Mcm-41 Mesoporous Materials for Dye Sensitized Solar Cell

I.R. Celine Rose

Department of Chemistry, Immaculate College for women, Cuddalore

Abstract

Mo-MCM-41, CdSe-MCM-41 and ZnSe-MCM-41 materials were synthesized by hydrothermal method. The synthesized materials were characterized by XRD, IR, SEM and N_2 adsorption – desorption isotherm. The efficiency of the materials was evaluated for photovoltaic performance. The powder X-ray diffraction revealed that the synthesized Mo-MCM-41, CdSe-Mo-MCM-41, ZnSe-Mo-MCM-41 mesoporous materials are hexagonal structure. Incorporation of Mo, CdSe and ZnSe into the framework decreases, the intensity of diffraction peaks, due to disordering of the mesoporous material. The nitrogen adsorption-desorption isotherms, a typical type III, IV and V isotherm was observed and due to capillary condensation in the mesopores. The surface area, pore size and pore volume were found to increase in CdSe and ZnSe functionalized MCM-41 materials. SEM images showed well-defined morphology in CdSe-Mo-MCM-41 and ZnSe-Mo-MCM-41. The fabrication of solar cell was carried out by Doctor Blade technique. Mesoporous materials such as Mo-MCM-41, CdSe-Mo-MCM-41 and ZnSe-Mo-MCM-41 were used as surface smoothing material in the fabrication of the counter electrode, to improve the life time of the counter electrode and it was found that efficiency of the mesoporous materials increases in the order Mo-MCM-41 < ZnSe-Mo-MCM-41 < CdSe-Mo-MCM-41.

Keywords: DSSC, Sensitizer, Mesoporous materials, Counter electrode.

Introduction

Dye-sensitized solar cells (DSSCs) are ability options to conventional silicon solar cells due to their low value, easy fabrication procedure and high energy conversion performance [1]. DSSC includes four components such as photoanode, an electrolyte, sensitizer and a counter electrode (CE). As one of the most vital components in DSSC, the CE collects electrons from the outside circuit and catalyzes the discount of triiodide ions to iodide ions. Platinum (Pt) is normally used as the CE fabric because of its correct conductivity for the delivery of electrons and amazing electro catalytic pastime for triiodide reduction [5], [6]. however, its excessive price and bad stability in corrosive I-/I3- redox gadget save you the massive-scale business software of DSSC in the future [7,8]. Carbonaceous materials are quite appealing and anticipated to be advanced as efficient electro catalysts for DSSCs because of their low cost, excessive catalytic activity, good electric conductivity and sturdy corrosion resistance. thus far, numerous carbon substances, together with carbon black [9], [10], activated carbon [11], [12], carbon nanotube [13], [14], [15], porous carbon [16], [17], and graphene [18], [19], [20], had been investigated

as CEs for DSSCs. however, in most instances, the catalytic activities of carbons are nonetheless not so good as that of Pt.

Efforts to improve the efficiency of the DSSC by giving importance in optimizing the various parameters that can affect the synthesis of nano II-VI semiconducting material were given in chapter III. As importance is given to the morphology of nanomaterials to improve the efficiency of the solar cell, which is not only depending upon the nature and morphology of semiconducting materials, as electrode but it depends on the mode of fabricating the solar cell. Though different methods like sputtering, chemical vapor deposition, spray pyrolysis, cathodic electrodeposition, spin coating, silar and Doctor Blade techniques are available for the fabrication of DSSC, the most economical way of fabrication method is considered [21].

In the literature survey, synthesis, characterisation (optical properties) of semiconducting functionalized mesoporous materials, especially II-VI semiconducting material (CdS) functionalized mesoporous MCM-41 was reported and highlighted the significance of these materials as it could be used as a electrode materials with high efficiency for fuel cell and battery [22], but the application of using semiconducting functionalized materials in photovoltaic cell, were not yet reported. As the semiconductors can act as guest in the host of silicate material, which is expected of acting as material for semiconductors against corrosion, abrasion resistance and prevapourized gas separation [23]. An attempt was made to synthesise, semiconducting functionalized mesoporous CdSe - / ZnSe - Mo-MCM-41 as counter electrodes to improve the efficiency of fabricated solar cell.

In the present work, Mo-MCM-41 type silicate materials were synthesized using cetyl trimethyl ammonium bromide, sodium silicate and ammonium molybdate by hydrothermal method and were characterized by powder X-Ray diffraction (XRD) techniques, Fourier transform Infrared (FT-IR) spectroscopy and Ultraviolet visible spectroscopy (UV-visible), scanning electron microscopy (SEM) and N_2 adsorption-desorption isotherm (BET). Additionally, the surface was functionalized by semiconducting nanoparticles (CdSe, ZnSe) through impregnation method. These surface functionalized mesoporous materials were applied as surface smoothing material as counter electrodes, to improve the life time of the counter electrodes in fabricating photovoltaic cell and to improve the efficiency of solar cell.

Experimental

Synthesis of CdSe nanoparticles

In the synthesis of CdSe, cadmium acetate and sodium selenite were taken in 1:1 ratio and were dissolved in 100 mL of deionized water by continuous stirring, followed by the addition of Ethylene glycol and hydrazine hydrate was added while stirring. Then the solution was refluxed under vigorous stirring at reaction temperature and reaction time which were optimized by carrying out the reaction at various temperature and reaction time. The precipitate was centrifuged at 3000 rpm for complete separation of CdSe nanoparticles. Finally, the precipitate was washed with ethanol and distilled water, then dried in vaccum at 100 ^{o}C for 18 h.

Synthesis of ZnSe nanoparticles

Nanoparticles of zinc selenide were synthesised by adapting the same procedure by using zinc acetate, selenous acid (1:1), deionised water, ethylene glycol and hydrazine hydrate in the volume ratio of 6:3:1 respectively.

Synthesis of Si-MCM-41 mesoporous material

The mesoporous Si-MCM-41 was synthesized by hydrothermal method using cetyltrimethylammonium

bromide (CTAB) and aq.NH3 as precursors. A solution of 16.4 g of CTAB was prepared by dissolving it in 49.2 g of deionised water. The mixture was heated at 75 °C to dissolve the CTAB. Then 9.5 g of aq. NH_3 was added followed by the addition of 10 g of tetraethyl orthosilicate (TEOS) slowly to the surfactant solution and stirred for 5 h at 30 °C. White precipitate was formed and washed with deionized water. Then it was dried at 90 ºC for 12 h followed by calcination at 500 ºC and kept at this temperature for 6h for complete removal of template.

Results and Discussion

X-ray diffraction Analysis

Powder X-ray diffraction patterns in the 2θ range of 1º to 8 º of mesoporous silicate, MCM-41 type materials, Mo-MCM-41, CdSe and ZnSe functionalized silicate materials are given in Figure 1, which reveals the existence of peak indexed to (100) (101) and (200), representing the ordered materials with hexagonal arrangement [28]. The intensity of the XRD peaks are found to be higher for Mo-MCM-41 than CdSe-Mo-MCM-41 and ZnSe-Mo-MCM-41 materials. Incorporation of molybdate, CdSe and ZnSe into the framework of silicate, the positions of the peaks of MCM-41, the intensity of diffraction peaks are gradually decreased due to the disordering of the mesopores .

The unit cell parameter (a_o) values for hexagonal Mo-MCM-41, CdSe-Mo-MCM-41 and ZnSe-Mo-MCM-41 material are calculated from the peak width of (100) plane by using the equation of $a_o = 2d_{(100)}\sqrt{3}$. In addition, the 'd' spacing value calculated using Bragg equation for all the materials are computed and corresponding data are summarized in Table 1.

The increase in d-spacing and unit cell parameter of CdSe-Mo-MCM-41, ZnSe- Mo-MCM-41 compared to Mo-MCM-41 suggests the presence of metal in the framework . It is also observed that the unit cell parameter and d_{100} spacing value increase with CdSe-Mo-MCM-41 and ZnSe-Mo-MCM-41.

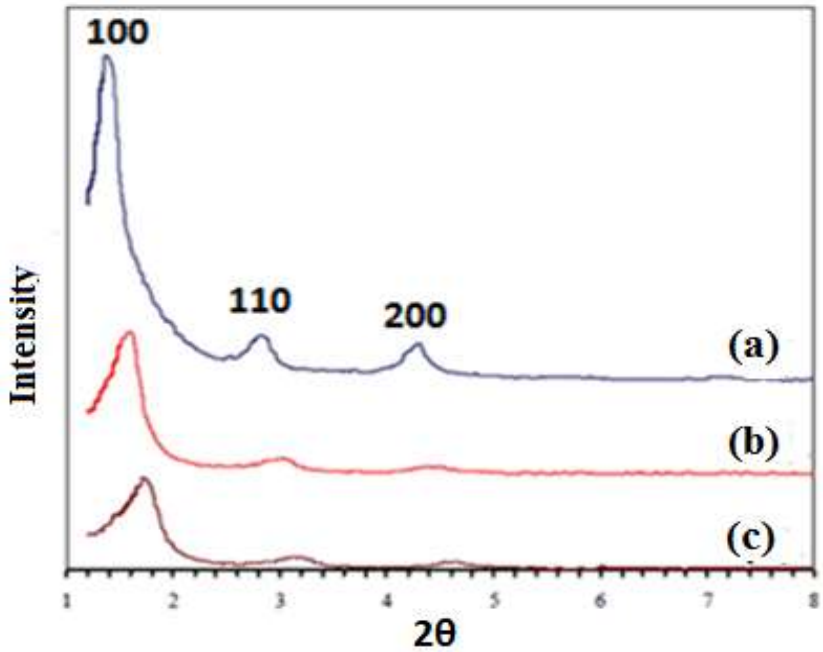

Fig. 1 XRD pattern of (a) Mo-MCM-41, (b) CdSe-Mo-MCM-41 and (c) ZnSe-Mo-MCM-41 materials

Table 1 The d-spacing and unit cell parameters of molybdate incorporated mesoporous materials

Samples	$d_{(100)}$ spacing (Å)	Unit cell parameters (a) (nm)
Mo-MCM-41	4.32	4.25
CdSe-Mo-MCM-41	4.36	4.28
ZnSe-Mo-MCM-41	4.43	4.94

BET analysis

The textural properties such as specific surface area, mesoporosity, pore volume and pore size distribution of mesoporous materials are studied by N_2 adsorption-desorption measurements and their values are included in Table 2. A typical nitrogen sorption isotherm of Mo-MCM-41, CdSe-Mo-MCM-41, ZnSe-Mo-MCM-41 material are illustrated in Figure 2, 3 and 4.

Table- 2 BET Analytical data of Mo-MCM-41 type materials.

Sample	Surface area (m^2/g)	Pore diameter (nm)	Total pore volume (cm^3/g)	Wall thickness (Å)	IUPAC classification	Remarks
Mo-MCM-41	594	2.6	0.6478	0.9	Type III isotherm	Mesoporous material
CdSe-Mo-MCM-41	620	2.86	0.728	0.6	Type IV isotherm	Mesoporous material
ZnSe-Mo-MCM-41	605	2.72	0.665	0.7	Type V isotherm	Mesoporous material

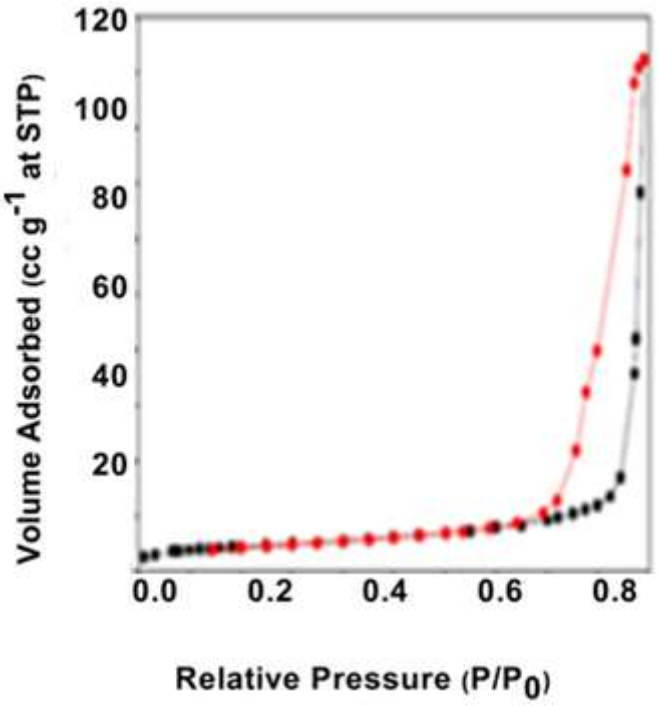

Fig. 2 N_2- adsorption-desorption isotherms of Mo-MCM-41 materials

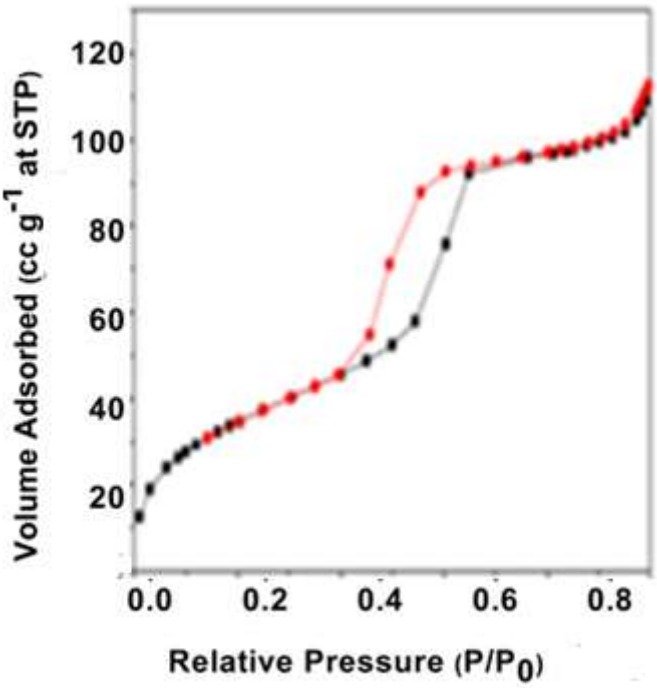

Fig. 3 N_2- adsorption-desorption isotherms of CdSe-Mo-MCM-41 materials

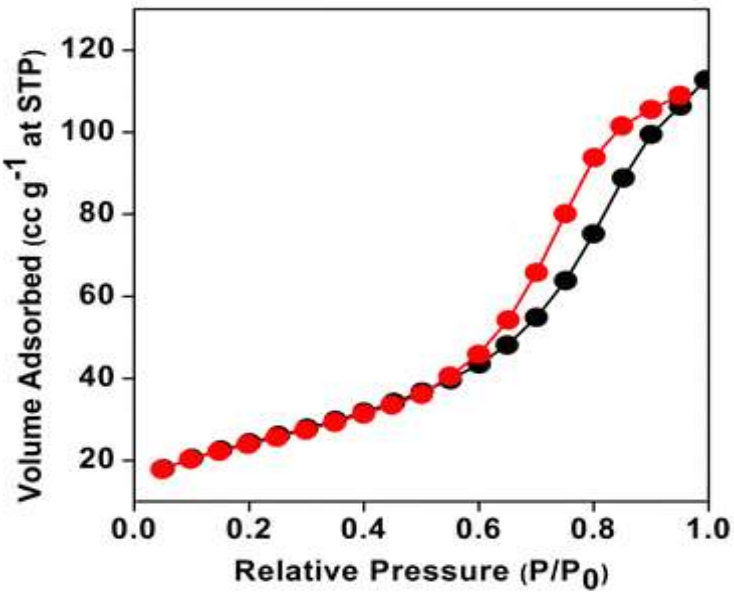

Fig. 4 N_2- adsorption-desorption isotherms of ZnSe-Mo-MCM-41 materials

Sample **Mo-MCM-41 is** exhibiting **Type III** isotherms. Samples CdSe-Mo-MCM-41 and ZnSe-Mo-MCM-41 exhibit Type IV and V isotherm which is a hysteresis loop typical for mesoporous materials. A significant change in the textural properties is seen on molybdenum incorporated mesoporous materials.

FT-IR (Fourier-Transform infrared spectroscopy)

The FT-IR spectroscopy of the synthesized Mo-MCM-41, CdSe-Mo-MCM-41 and ZnSe-Mo-MCM-41 samples were recorded between 4000 and 500 cm^{-1}**.** The obtained frequency and their vibration bands are

Si-OH, Si-O, Si-H, Si-C, C-O and OH bonds are given in Figure 5. The broad IR bands around 3500 cm^{-1} are assigned to the water molecules. The absorption band at 1084 cm^{-1} are due to the Si-O-Si bridges. The absorption band at 806 cm^{-1} is due to the M-M bending vibration. A band at 453 cm^{-1} is showed as visible spectra, which is assigned to the framework of metal- metal stretching vibration**.**

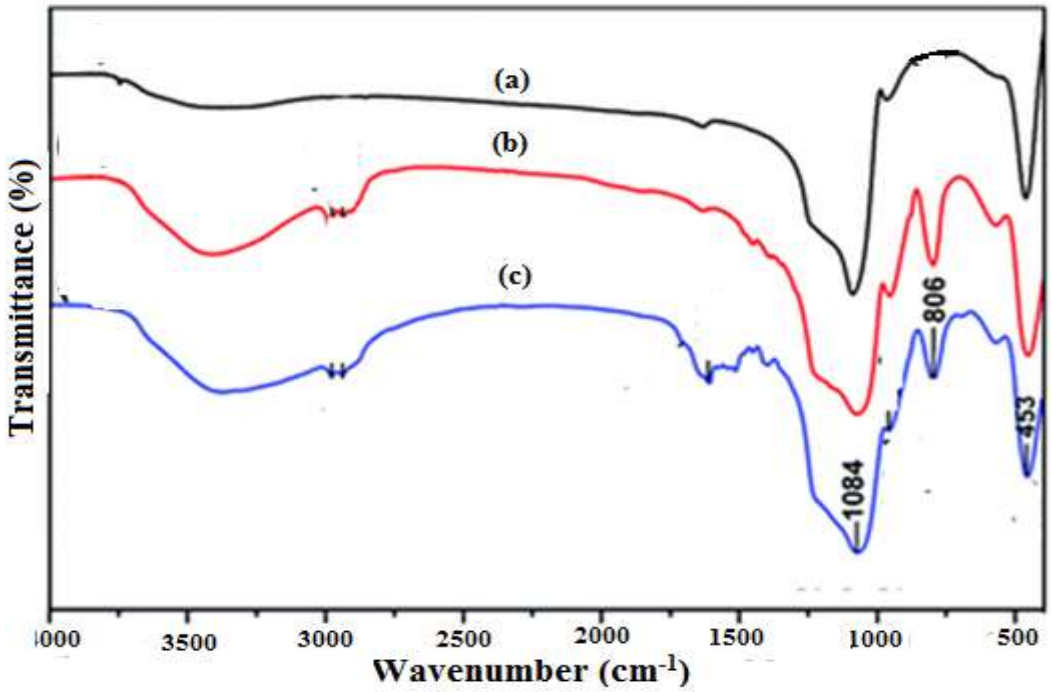

Fig. 5 FT-IR spectra of (a) Mo-MCM-41, (b) ZnSe-Mo-MCM-41 and (c) CdSe-Mo-MCM-41 catalysts

Scanning Electron Microscopic analysis

The surface morphology of the materials is studied by scanning electron microscope and the images are shown in Figure 6. The SEM images of Mo-MCM-41, ZnSe-Mo-MCM-41 and CdSe-Mo-MCM-41 material are of well defined spherical structures. The aggregated spherical like particles are shown by Mo-MCM-41. The surface morphology of the CdSe-Mo-MCM-41and ZnSe-Mo-MCM-41 attain more orderly arrangement.

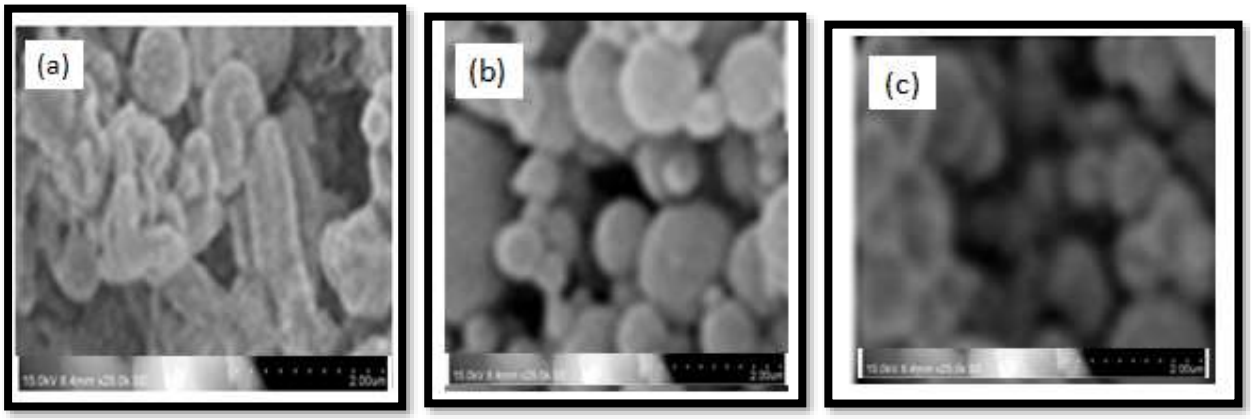

Fig. 6 SEM images of synthesized catalyst (a) Mo-MCM-41 (b) CdSe-Mo-MCM-41 (c) ZnSe-Mo-MCM-41

X-ray Photoelectron Spectroscopy

XPS spectra of CdSe-Mo-MCM-41 composites are recorded and core level photo electron peaks of O 1s, $Si2p_{3/2}$, $Mop_{3/2}$, $Mop_{1/2}$ Cd $3d_{5/2}$ and Cd $3d_{3/2}$ are shown individually in each Figures 7 [a,b,c,d,e]. The peak at 104.1 eV is attributed to the SiO_2 of MCM-41 and 532.5 eV for the binding energy of O 1s . The XPS spectra of molybdenum show peak in the range of 390-420 eV. Binding energy of $Mo3p_{1/2}$ lies in the range of 415-420 and 395- 405 for the binding energy value of $Mo3p_{3/2}$. It observed and due to the probable conclusion that Cd atoms or Se atoms or both will interact with the silanol groups of MCM-41 and to form Si-O-Cd or Si-O-Se bonds.

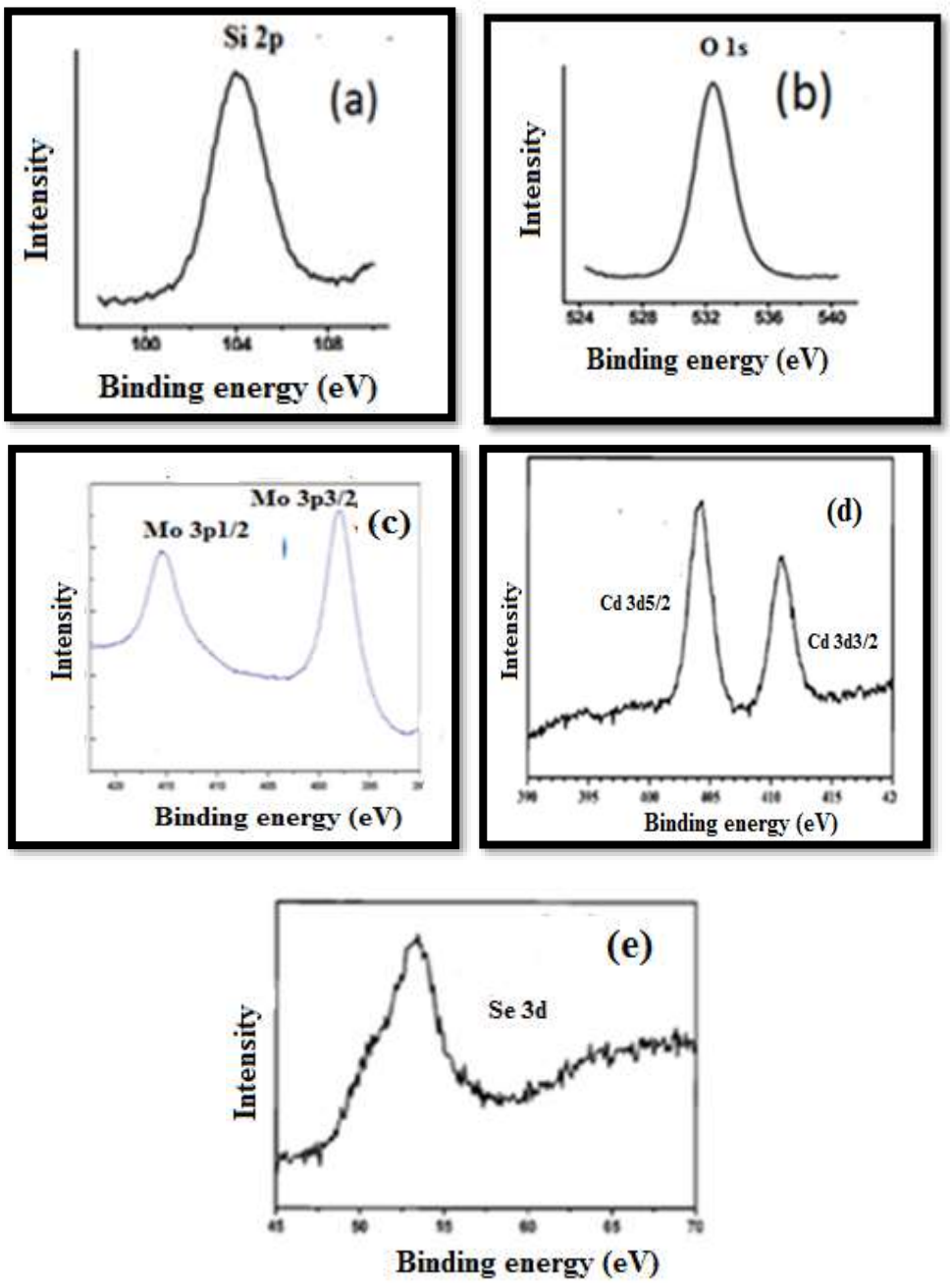

Fig. 7 X-ray photo electron spectra of CdSe-Mo-MCM-41 a) Si 2p b) O 1s c) Mo 3p d) Cd 3d and e) Se 3d peaks.

Table 3 photo electron peaks and binding energy values of CdSe-Mo-MCM-41 material.

Material	Photo electron peaks	Binding energy
CdSe-Mo-MCM-41	O1s	104.1 eV
	Si 2p3/2	532.5 eV
	Mo p3/2	415-420 eV
	Mo p1/2	395-405 eV
	Cd 3d5/2	404.3 eV
	Cd 3d5/2	410.9 eV
	Se 3d	53.4 eV

4.6 Photovoltaic Studies:

The photovoltaic performance of the fabricated DSSC using Mo-MCM-41, CdSe-Mo-MCM-41 and ZnSe-Mo-MCM-41 as photocathodes, sensitized TiO_2 photoanode were studied by the J-V characteristics studies under the illumination of light with 1 sun intensity (Fig. 8).

The J-V characteristics curves show a poor photovoltaic response for Mo-MCM-41 mesoporous materials sensitized TiO_2 photoelectrodes (η= 0.99 %) due to the poor conducting nature of MCM mesoporous materials. The short circuit current for Mo-MCM mesoporous materials sensitized TiO_2 electrode (Jsc = 0.72 mA) was gradually increased by the sensitization of CdSe-Mo-MCM-41 mesoporous materials. The increase of Jsc is attributed to the enhanced optical properties of the CdSe-Mo-MCM-41 and ZnSe-Mo-MCM-41 mesoporous materials. While incorporated with Mo, CdSe, ZnSe, more light was utilized to generate the photoelectrons resulting in the increment of Jsc which inturn increased the Voc.

The improved efficiency of 0.99, 4.51 and 6.21% were achieved for Mo-MCM-41, ZnSe-Mo-MCM-41, CdSe-Mo-MCM-41 for the fabricated DSSC respectively, and supported that CdSe-Mo-MCM-41, and ZnSe-Mo-MCM-41 could be used as the potential photocathodes in DSSC for enhanced photoconversion efficiency.

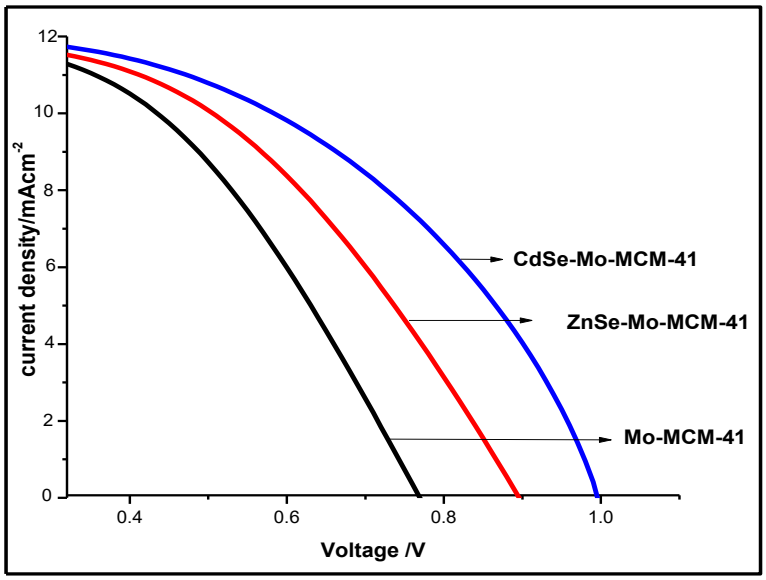

Fig. 8 Current density-voltage (J-V) of Mo-MCM-41, CdSe-Mo-MCM-41 and ZnSe-Mo-MCM-41

Table 4 Photovoltaic performance of Mo-MCM-41, CdSe-Mo-MCM-41 and ZnSe-Mo-MCM-41

Parameters	Mo-MCM-41	CdSe-Mo-MCM-41	ZnSe-Mo-MCM-41
Voc [V]	11.2	11.8	11.3
Jsc [mA/cm^2]	0.72	1.0	0.9
FF	0.6091	0.6686	0.6229
η [%]	0.99	6.21	4.51

Mo-MCM-41, CdSe-MCM-41 and ZnSe-MCM-41 materials were synthesized by hydrothermal method . The synthesized materials were characterized by XRD, IR, SEM and N_2 adsorption – desorption isotherm. The efficiency of the materials was evaluated for photovoltaic performance. The powder X-ray diffraction revealed that the synthesized Mo-MCM-41, CdSe-Mo-MCM-41, ZnSe-Mo-MCM-41 mesoporous materials are hexagonal structure. Incorporation of Mo, CdSe and ZnSe into the framework decreases, the intensity of diffraction peaks, due to disordering of the mesoporous material . The nitrogen adsorption-desorption isotherms, a typical type III, IV and V isotherm with a hysteresis loop was observed and confirm the mesopores of the materials. The surface area, pore size and pore volume were found to increase in CdSe and ZnSe functionalized MCM-41 materials. SEM images showed well-defined morphology in CdSe-Mo-MCM-41 and ZnSe-Mo-MCM-41. The fabrication of solar cell was carried out by Doctor Blade technique. Mesoporous materials such as Mo-MCM-41, CdSe-Mo-MCM-41 and ZnSe-Mo-MCM-41 were used as surface smoothing material in the fabrication of the counter electrode, to improve the life time of the counter electrode and it was found that efficiency of the mesoporous materials increases in the order Mo-MCM-41 < ZnSe-Mo-MCM-41 < CdSe-Mo-MCM-41.

Conclusion

CdSe and ZnSe nanoparticles functionalized MCM-41 mesoporous materials and part II deals with the CdSe and ZnSe nanoparticles functionalized SBA-15 mesoporous materials. The inorganic polymeracts as a binder and smoothens the surface of the fabrication, which further increases the efficiency of solar cell. The maximum efficiency was obtained for the dye sensitized solar cell fabricated with CdSe-MCM-41 (6.21 %) and CdSe -SBA-15 (5.98%).

References

1. Satyajit Saha," Structural and Optical Properties of Chemically Grown CdSe Nanoparticles", Journal of Physical Sciences, Vol. 15, 251-254, 2011.
2. C. B. Murray, D. J. Norris, and M. G. Bawendi, "Synthesisand characterization of nearly monodisperse CdE (E = S, Se,Te) semiconductor nanocrystallites," Journal of the American Chemical Society, vol. 115, 8706–8715, 1993.
3. Sreekumaran Nair,Zhu Peining,V. Jagadeesh Babu,Yang Shengyuanc and Seeram Ramakrishnab", Anisotropic TiO2 nanomaterials in dyesensitized solar cells", Phys. Chem. Chem. Phys., Vol 13, pp. 21248–21261,2011.
4. Y.-L. Lee and C.-H. Chang, "Efficient polysulfide electrolyte for CdS quantum dot-sensitized solar cells," Journal of Power Sources, vol. 185, pp. 584–588, 2008.
5. H. Wang, Y. Bai, H. Zhang, Z. Zhang, J. Li, and L. Guo, "CdS quantum dots-sensitized TiO_2 nanorod array on transparent conductive glass photoelectrodes," Journal of Physical Chemistry C, vol. 114, pp. 16451–16455, 2010.

6. Y.-L. Lee, C.-F. Chi, and S.-Y. Liau, "CdS/CdSe co-sensitized TiO_2 photoelectrode for efficient hydrogen generation in a photoelectrochemical cell," Chemistry of Materials, vol. 22, pp. 922–927, 2010.
7. H. S. Chen, C. Su, J. L. Chen, T. Y. Yang, N. M. Hsu, and W. R. Li, "Preparation and characterization of pure rutile TiO2 nanoparticles for photocatalytic study and thin films for dye-sensitized solar cells," Journal of Nanomaterials, vol. 2011, Article ID 869618, pp.8, 2011.
8. M. Sun, G. Chen, Y. Zhang, Q. Wei, Z. Ma, and B. Du, "Efficient degradation of azo dyes over Sb2S3/TiO2 heterojunction under visible light irradiation," Industrial & Engineering Chemistry Research, vol. 51, pp. 2897–2903, 2012.
9. P. K. Santra and P. V. Kamat, "Mn-doped quantum dot sensitized solar cells: a strategy to boost efficiency over 5%," Journal of the American Chemical Society, vol. 134, pp. 2508–2511, 2012.
10. D. Mocatta, G. Cohen, J. Schattner, O. Millo, E. Rabani, andU. Banin, "Heavily doped semiconductor nanocrystal quantumdots," Science, vol. 332, pp. 77–81, 2011.
11. V. Chikan, "Challenges and prospects of electronic doping of colloidal quantum dots: case study of CdSe," The Journal of Physical Chemistry Letters, vol. 2, pp. 2783–2789, 2011.
12. Gholam Reza Amiri1, Soheil Fatahian, Somayeh ahmoudi, "Preparation and Optical Properties Assessment of CdSe Quantum Dots",Materials Sciences and Applications, Vol. 4, pp 134-137, 2013.
13. W. A. Tisdale, K. J.Williams, B. A. Timp,D. J.Norris,E. S.Aydil,and X.-Y. Zhu, "Hot-electron transfer from semiconductornanocrystals," Science, vol. 328, pp.1543–1547, 2010.
14. Santanu, T. Christopher, F. Fadzai, D. Pinar, and C. Viktor,"Progress toward producing n-type CdSe quantum dots: tin and indium doped CdSe quantum dots," Journal of Physical Chemistry C, vol. 113, pp. 13008–13015, 2009.
15. J.W. Lee, D. Y. Son, T. K. Ahn et al., "Quantum-dot-sensitized solar cell with unprecedentedly high photocurrent," ScientificReports, vol. 3, article 1050, 2013.
16. H.Wang, B. H.Wang, Y. X. Hu et al., "A method for Co-doped CdSe quantum-dot sensitized TiO2 nano-rod photo-electrodeand its preparation method," China Patent, Application Number 201210234979, July 2012.
17. P. K. Santra and P. V. Kamat, "Mn-doped quantum dot sensitized solar cells: a strategy to boost efficiency over 5%," Journal of the American Chemical Society, vol. 134, pp. 2508–2511, 2012.
18. H. Wang, Y. Bai, H. Zhang, Z. Zhang, J. Li, and L. Guo, "CdS quantum dots-sensitized TiO_2 nanorod array on transparent conductive glass photoelectrodes," Journal of Physical Chemistry C, vol. 114, pp. 16451–16455, 2010
19. S. Tiwari and S. Tiwari, "Development of CdS based stable thin film photo electrochemical solar cells," Solar Energy Materials and Solar Cells, vol.90, pp. 1621–1628, 2006.
20. P. K. Santra and P. V. Kamat, "Mn-doped quantum dot sensitized solar cells: a strategy to boost efficiency over 5%," Journal of the American Chemical Society, vol.134, pp. 2508–2511, 2012.
21. F. A. de Castro, F. Nüesch, C. Walder, and R. Hany, "Challenges found when patterning semiconducting polymers with electric fields for organic solar cell applications," Journal of Nanomaterials, vol. 2012, Article ID 478296, pp.6, 2012.
22. U. Farva and C. Park, "Colloidal synthesis and air-annealing of CdSe nanorods for the applications in hybrid bulk hetero-junction solar cells," Materials Letters, vol.64, pp. 1415–1417, 2010.

23. L. M. Peter, K. G. U. Wijayantha, D. J. Riley, and J. P. Waggett, "Band-edge tuning in self-assembled layers of Bi2S3 nanoparticles used to photosensitize nanocrystalline TiO2," Journal of Physical Chemistry B, vol. 107, no. 33, pp. 8378–8381, 2003.
24. L. Liu, J. Hensel, R. C. Fitzmorris, Y. Li, and J. Z. Zhang, "Preparation and photoelectrochemical properties of CdSe/TiO2 hybrid mesoporous structures," Journal of Physical Chemistry Letters, vol. 1, pp. 155–160, 2010
25. A.Jeya Rajendran, M.Prabhu, K.EswaraMoorthi, I.R.Celine Rose, Santhanaraj, Alison Frenandaz, Sugandhi, Radhika, **"**Dielectric and conductivity studies Stereoselectively synthesised of d- and l- nor-ephedrine" J Therm Anal Calorim, vol. 118, 2014.
26. P.V.Kamat, "Nanostructure Architectures for Solar EnergyConversion, "J.Phys.Chem. 2834–2860, 2007.
27. C.F. Chi, H.W. Cho, H. Teng et al., "Energy level alignment,electron injection, and charge recombination characteristics in CdS/CdSe cosensitized TiO2 photoelectrode," Applied Physics Letters, vol. 98, Article ID 012101, 2011.
28. S. Jana, B. B. Srivastava, and N. Pradhan, "Correlation of dopant states and host bandgap in dual-doped semiconductor nanocrystals,"The Journal of Physical Chemistry Letters, vol. 2, pp. 1747–1752, 2011.
29. Hee.Je.Kim, S.N.Karthick "Curcumin dye extracted from curcuma longa L used as sensitizers for efficient dye-sensitized solar cells"' Int.J.Electrochem.sci, vol.8,8320-8328, 2013.